

# Geometrical and electronic structures of the (5, 3) single-walled gold nanotube from first-principles calculations

Xiaoping Yang

*Group of Computational Condensed Matter Physics,  
National Laboratory of Solid State Microstructures and Department of Physics,  
Nanjing University, Nanjing 210093, P. R. China and*

*Department of Physics, Huainan Normal University,  
Huainan, Anhui 232001, P. R. China*

Jinming Dong

*Group of Computational Condensed Matter Physics,  
National Laboratory of Solid State Microstructures and Department of Physics,  
Nanjing University, Nanjing 210093, P. R. China*

## Abstract

The geometrical and electronic structures of the 4 Å diameter perfect and deformed (5, 3) single-walled gold nanotube (SWGT) have been studied based upon the density-functional theory in the local-density approximation (LDA). The calculated relaxed geometries show clearly significant deviations from those of the ideally rolled triangular gold sheet. It is found that the different strains have different effects on the electronic structures and density of states of the SWGTs. And the small shear strain can reduce the binding energy per gold atom of the deformed SWGT, which is consistent with the experimentally observed result. Finally, we found the finite SWGT can show the metal-semiconductor transition.

PACS numbers: 73.22.-f, 61.46.+w, 73.63.Nm

Nanowires and nanotubes have raised extensive interest, which is motivated both by their special electrical and mechanical properties as well as by their potential applications in future nanostructure materials. For example, the unique electronic and mechanical properties of carbon nanotube (CNT) [1-4] are proved to be a rich source of new fundamental physics and also a promising candidate of nanoscale wires, transistors and sensors. So, the cylindrical tubes and nanowires made of other materials are also the subject of intense researches. For example, Si, BN, SiSe<sub>2</sub>, WS<sub>2</sub>, MoS<sub>2</sub>, NiCl<sub>2</sub>, and various metallic nanowires [5], e.g., gold nanowires, are experimentally studied [6].

The long gold nanowires with diameter less than 2 nm have been experimentally synthesized in an ultra-high vacuum (UHV) — transmission electron microscope (TEM) with the electron-beam thinning technique [7], showing a coaxial helical multishell (HMS) structure, which is similar to that of the multiwalled CNT except that the honeycomb network of carbon atoms in the CNT is replaced by a triangular network of gold atoms (Fig. 1) [7-10]. The triangular network can be deformed due to the shear strain  $\varepsilon$  caused by the metallic bond. A helical double walled  $n$ - $n'$  gold nanowire is composed of two coaxial tubes with  $n$  and  $n'$  helical gold atomic rows in the outer and inner tube, respectively, which coiled round the tube axis. It is found that the inner and outer shells always have even-odd or odd-even coupling, and the difference  $(n - n')$  between their number of atomic row is equal to seven (a single atom chain is regarded as "0"-membered in this discussion). Nanowires with  $n \leq 6$  had been supposed to have only a single-walled shell [7], called as SWGT, which has recently been synthesized experimentally at 150 K in an UHV—TEM [11]. The thinnest SWGT, 4 Å in diameter, was found to be the (5, 3), composed of five atomic rows coiled round the tube axis.

The geometrical structure of the SWGT is schematically shown in Fig. 1(a), where  $\vec{a}_1$  and  $\vec{a}_2$  denote two basis vectors of the triangular network. The triangular network is deformed by the shear strain  $\varepsilon$  in  $\vec{a}_2$  direction. The tube unit cell is defined by the vector  $\vec{C}(n, m) = n\vec{a}_1 + (m + n\varepsilon/2)\vec{a}_2$  and its orthogonal  $\vec{OB}$  parallel to the tube axis. As used in the single-walled carbon nanotube (SWNT), here, a pair of integers,  $(n, m)$ , is also used to represent a SWGT consisting of  $n$  close-packed atomic rows with a helical angle ranging from  $0^\circ$  ( $m = n/2$ ) to  $30^\circ$  ( $m = 0$ ), which is defined as the angle between the atom row and the tube axis.

It is well known that a mechanical deformation of a SWNT affects heavily its electronic structures [12-14]. So, it is natural to ask what happens for the SWGT due to different deformations. In this paper, we use the first-principles calculation to study the structural and electronic properties of the 4 Å diameter SWGT (5, 3) exerted by three kinds of strains, i.e. the uniaxial stretch, torsional and shear strains. In addition, we investigate the effect of the finite length of SWGT on its electronic structures.

The total energy plane-wave pseudopotential method [15] has been used in our calculations within the framework of local density approximation (LDA). The ion-electron interaction is modeled by ultra-soft local pseudopotentials of the Vanderbilt form [16] with a uniform energy cutoff of 224.7 eV. There are 21 uniformly distributed  $k$  points along the nanotube symmetry axis  $\Gamma X$ . The supercell geometry for the SWGT has been used [17], in which the tubes are aligned in a hexagonal array with the closest distance between the adjacent tubes being 20 Å, larger enough to prevent the tube-tube interactions. Using the same computational method, we have also calculated the band structure of the SWGT (8, 4) plus one atomic row at the center of the tube, and the obtained result is well consistent with that in Ref. [8].

Firstly, we study the structural and electronic properties of the fully relaxed perfect SWGT (5, 3) and a uniaxially stretched one (with uniaxial strain of 0.05 and 0.1), for which the obtained structure parameters are shown in Table I. From it we can find that the diameter of the relaxed perfect (5, 3) tube is 0.2 Å larger than that (4.03 Å) of ideal tube rolled up from the gold triangular network sheet, while its lattice constant along the tube axis is 1.137 Å smaller than that (21.895 Å) of an ideal tube. This is due to the curvature effect that weakens the bonds that are wrapping around the circumference of the tube. So, it is also found that the average bond length along the axis of relaxed perfect tube is shorter than those in the direction of the circumference. However, under the uniaxial strain of 0.05 and 0.1, the diameter of the deformed tube gradually recovers that of the ideal tube. In addition, the binding energy per gold atom for the uniaxial stretched tube is obviously found to be higher than that of the relaxed perfect tube.

The calculated electronic band structures and density of states are shown in Fig. 2(a)-2(c) and 3(a)-3(b) (only the DOSs of the uniaxial stretch strain of 0.1 are given as an example for the case of the uniaxial stretch), respectively. Comparing Fig. 2(a) with 2(b) and 2(c), we can find that the uniaxial stretch strain makes the bands near the Fermi level move toward the higher energy, but keeping always five conduction channels on the Fermi level. So, the SWGT (5, 3) is not affected sensitively by the uniaxial strain. And the shifts of the energy bands lead to the shifts of the DOS peaks, which can be seen clearly in Fig. 3(a) and (b). Three DOS peaks at -1.74, -0.15 and 1.76 eV (Fig. 3(a)) are blue-shifted to -1.71, 0.03 and 1.86 eV under uniaxial strain of 0.1, respectively (Fig. 3(b)). At the same time, the DOS peak at -1.92 eV (Fig. 3(a)) in valence band is red-shifted to -2.01 eV (Fig. 3(b)). The uniaxial stretch of 0.1 leads also to disappearance of the DOS peak at -1.32 eV (Fig. 3(a)) in Fig. 3(b).

Secondly, we have studied the geometrical structures and electronic properties of the torsionally deformed SWGT (5, 3), whose ball-and-stick pictures are also shown in Fig. 1. When the torsional strain takes positive  $+4.302^\circ$  or negative  $-6.562^\circ$ , it means the strain is applied along CB (OA) or BC (AO) direction in Fig. 1(a). The obtained structural parameters of the fully relaxed tubes are shown in Table I too, from which it is found that the diameters of the both deformed (5, 3) tubes are larger than that of the perfect one. The positive torsion makes the strained bond  $b$  (and  $a$ ) longer (shorter) than that without the strain; while the negative torsion leads to a reverse case. Meanwhile, the strained bond  $c$  always becomes shorter than that before with different torsional strains. The binding energies per gold atom under the positive and negative torsions are larger than that of perfect tube by maximal 0.031 eV.

The calculated electronic band structures and density of states are shown in Fig. 2(d), 2(e) and Fig. 3(c) (choose only the torsional strain of  $+4.302^\circ$  as an example). Since the total gold atom numbers are 23 and 5 per unit cell under the torsional strains of  $+4.302^\circ$  and  $-6.562^\circ$ , respectively, some energy bands clearly disappear in Fig. 2(d) and 2(e), especially for the negative  $-6.562^\circ$ . But they still keep five conduction channels on the Fermi level, which clearly indicates the torsional strain does not affect more heavily the SWGT (5, 3) than the uniaxial one. The complex change of the energy bands makes the shift of DOS peaks different from that under the uniaxial stretch strain. Under the torsional strain of  $+4.302^\circ$ , the three DOS peaks at -1.92, -1.32 and -0.15 eV in Fig. 3(a) are red-shifted to -1.93, -1.48 and -0.22 eV, respectively in Fig. 3(c), and DOS peaks at -1.74 and 1.76 eV in Fig. 3(a) are blue-shifted to -1.71 and 1.85 eV in Fig. 3(c), respectively.

Finally, we study the structural and electronic properties of deformed SWGT (5, 3) under

shear strain. Due to limitation of the computational time and cost, we can only select the shear strain of  $\varepsilon = 0.0314$  along the basis vector  $\vec{a}_2$  (Fig. 1(a)), making the one unit cell of the deformed tube contain 33 gold atoms, which is schematically shown in Fig. 1. The obtained fully relaxed structure parameters are shown in Table I too, and from it we can find that the diameter of the shear-strain deformed SWGT (5, 3) is only slightly larger than that of the perfect one. But its binding energy per gold atom is smaller than that of perfect tube by 0.008 eV, which means it is more stable than the perfect tube, being consistent with the experimentally observed result [11]. Its calculated electronic band structures and DOSs are shown in Fig. 2(f) and Fig. 3(d). Comparing Fig. 2(f) with Fig. 2(a), we can find the shear strain of 0.0314 causes less change of the band structure since its total atom number per unit cell is 33, only 5 less than that (38) of the perfect tube, and only a few bands disappear. So, the conduction channel on the Fermi level still remains five. As for its DOSs, we found three DOS peaks at -1.92, -1.32 and -0.15 eV in Fig. 3(a) are slightly red-shifted to -1.93, -1.36 and -0.17 eV in Fig. 3(d), respectively, and only the DOS peak at 1.76 eV in Fig. 3(a) is slightly blue-shifted to 1.78 eV in Fig. 3(d). Meanwhile, the peak position at -1.74 eV in Fig. 3(a) is not changed, but its height is decreased. And a new weaker DOS peak emerges at -1.55 eV in Fig. 3(d), which corresponds to the shoulder between the DOS peak values -1.74 and -1.32 eV in Fig. 3(a). Experimentally, the synthesized SWGT (5, 3) has an intrinsic shear strain  $\varepsilon$  of 0.005, which is far smaller than that used in our calculation. So, based on our result the shear strain effect on the electronic structure of the SWGTs should be very small. In addition, we found that the deformed (5, 3) tubes under the torsional strain of  $1.006^\circ$  and shear strain of 0.0314 have the very similar structural parameters (see Table 1) and the electronic structures. And the difference between their DOS peak positions is also small, lying in a range of about  $\pm 0.04$  eV, which indicates that the very small shear strain plays an equivalent role in the SWGT (5, 3) as a torsional strain.

In addition, it is noted from Fig. 3 that the DOS peaks in valence bands lower than -0.5 eV are mainly contributed by the *d*-orbital electrons; while the *s*-orbital electrons dominate the energy bands higher than -0.5 eV, which is similar for the deformed tubes under three different kinds of strains.

In addition to the SWGT (5, 3), we also study the electronic properties of the deformed SWGT (5, 0) (helical angle is  $30^\circ$ ) and SWGT (6, 3) (helical angle is  $0^\circ$ ) under the similar uniaxial stretch of 0.1 and torsional strains ( $+4.715^\circ$  for (5, 0) and  $+6.587^\circ$  for (6, 3)). The band structures of (5, 0) and (6, 3) are shown in Fig. 4. It can be seen in Fig. 4 that no significant changes are found, and the Fermi level in every panel is always crossed by five conduction bands (the two-degenerate state is labeled by the arrow). Under the uniaxial strain, the energy bands near the Fermi level move toward the higher energy area, and the torsional strain eliminate the double-degeneracy of the energy band near the Fermi level. The different changes of the energy bands under the two kinds of the strains make inevitably the shift of the DOS peaks different, which is consistent with the above results of SWGT (5, 3). It is found that the SWGT (6, 3) has the same five conduction channels as (5, 3) and (5, 0) tubes indicating clearly no direct correlation between the numbers of the atom rows and the conduction channels.

It is known that most of the deformed SWNTs show a metal-semiconductor transition (MST), occurring periodically with increasing strain [18-20], but why do the deformed SWGTs always remain metal? There are two inequivalent carbon atoms in one unit cell of the hexagonal graphite sheet, causing both of bonding and anti-bonding bands, which cross at six points, and so are easy to be separated by applied strains. In contrast, only

one gold atom exists in one unit cell of the triangular gold sheet, leading to only one energy band. So, the uniaxial and torsional strain can not make the periodic infinite SWGT show the MST, which is already proved by the above calculated results. However, the practical SWGTs have the finite length of usual several nanometers (Ref. 11), and so it is necessary to study the finite length effect on the physical properties of SWGT. Our numerical calculation indicates that the SWGT (5, 3) with a length of 4.15 nm (about two times larger than the perfect tube period) shows the characteristic of the semiconductor with its gap of 0.11 eV. And it is found the energy gap will oscillate with increasing length, which is similar to that of SWNT [21-22]. Due to limitation of computation time, we take only the results of SWGT (5, 0) as an example in Table II, from which we know the SWGT (5, 0) with the optimized length of about 1.37, 1.83, 2.29, 3.2 and 3.67 nm have the energy gap of 0.75, 0.3, 0.16, 0.23 and 0.165 eV, respectively, but the ones with the optimized length of 2.75 and 4.12 nm remain metal. Therefore, by applied strains, the finite-length SWGT can also show the similar MST as the SWNT.

In summary, we have systematically studied the structural and electronic properties of the perfect and deformed SWGT (5, 3), under three kinds of strains, i.e. the uniaxial stretch, torsional and shear strains. It is found that there is no direct correlation between number of the atom rows forming the SWGT and that of conduction channels, and it is difficult to change the conduction channel number under the applied strains, which always keeps five. The small shear strain can reduce the binding energy per gold atom of SWGT, which is consistent with the experimentally observed result. Compared with the SWNT, the geometrical and electronic structures of the SWGT are more stable under the applied strains, making absent the MST for the deformed infinite SWGT, which contrasts to those in SWNT. However, the SWGT with the finite length is found to show the characteristic of the semiconductor. We hope the obtained results in this paper will be helpful to design nanoscale electronic device based on the SWGT.

This work was supported by the Natural Science Foundation of China under Grant No. 10474035, No. A040108, and also support from a Grant for State Key program of China through Grant No. 2004CB619004.

- 
- <sup>1</sup> S. Iijima, *Nature (London)* **354**, 56 (1991).
  - <sup>2</sup> T.W. Ebbesen, P.M. Ajayan, *Nature (London)* **358**, 220 (1992); J. Kong, H.T. Soh, A.M. Cassell, C.F. Quate, H. Dai, *Nature (London)* **395**, 878 (1998).
  - <sup>3</sup> M. Endo, K. Takeuchi, K. Kobori, K. Takahashi, H.W. Kroto, A. Sarkar, *Carbon* **33**, 873 (1995).
  - <sup>4</sup> L.C. Qin, S. Iijima, *Mater. Lett.* **30**, 311 (1997).
  - <sup>5</sup> O. Gülseren, F. Ercolessi, and E. Tosatti, *Phys. Rev. Lett.* **80**, 3775 (1998).
  - <sup>6</sup> M.S. Dresselhaus, G. Dresselhaus, Ph. Avouris, editors. *Carbon nanotubes*. Berlin: Springer, 2001.
  - <sup>7</sup> Y. Kondo and K. Takayanagi, *Science* **289**, 606 (2000).
  - <sup>8</sup> E. Tosatti, S. Prestipino, S. Kostlmeier, A. Dal Corso, F.D. Di Tolla, *Science* **291**, 288 (2001).
  - <sup>9</sup> Y. Oshima, Y. Kondo, and K. Takayanagi, *J. Electron Microsc.* **52**, 49 (2003).
  - <sup>10</sup> R.T. Senger, S. Dag and S. Ciraci, *Phys. Rev. Lett.* **93**, 196807 (2004).
  - <sup>11</sup> Y. Oshima, A. Onga and K. Takayanagi, *Phys. Rev. Lett.* **91**, 205503 (2003).
  - <sup>12</sup> T.W. Tombler, C. Zhou, L. Alexseyev, J. Kong, H. Dai, L. Liu, C.S. Jayanthi, M. Tang, S. Wu, *Nature (London)* **405**, 769 (2000).

- <sup>13</sup> A. Maiti, A. Svizhenko, M.P. Anantram, Phys. Rev. Lett. **88**, 126805 (2002); E.D. Minot, Y. Yaish, V. Sazonova, J.Y. Park, M. Brink, P.L. McEuen, *ibid.* **90**, 156401 (2003).
- <sup>14</sup> J. Cao, Q. Wang, H. Dai, Phys. Rev. Lett. **90** 157601 (2003); M.B. Nardelli, J. Bernholc, Phys. Rev. B **60**, R16338 (1999).
- <sup>15</sup> the Vienna *ab initio* simulation package (VASP): G. Kresse and J. Hafner, Phys. Rev. B **47**, 558 (1993); G. Kresse and J. Furthmuller, *ibid.* **54**, 11169 (1996).
- <sup>16</sup> A.M. Rappe, K.M. Rabe, E. Kaxiras, J.D. Joannopoulos, Phys. Rev. B **41**, 1227-1230 (1990).
- <sup>17</sup> X. Blase, L.X. Benedict, E.L. Shirley, S.G. Louie, Phys. Rev. Lett. **72**, 1878 (1994).
- <sup>18</sup> R. Heyd, A. Charlier, E. McRae, Phys. Rev. B **55**, 6820 (1997); L. Yang, M.P. Anantram, J. Han, J.P. Lu, *ibid.* **60**, 13874 (1999).
- <sup>19</sup> D.W. Brenner, J.D. Schall, J.P. Mewkill, D.A. shenderova, S.B. Sinnott, Interplanet. Soc. **51**, 137 (1998).
- <sup>20</sup> C.L. Kane, E.J. Mele, Phys. Rev. Lett. **78**, 1932 (1997); L. Yang, J. Han, *ibid.* **85**, 154 (2000).
- <sup>21</sup> A. Rubio, D. Sanchez-Portal, E. Artacho, P. Ordejón, and J. M. Soler, Phys. Rev. Lett. **82**, 3520 (1999).
- <sup>22</sup> J. Jiang, J. Dong and D.Y. Xing, Phys. Rev. B **65**, 245418 (2002); H. Jiang, G. Wu, X.P. Yang and J. Dong, *ibid.* **70**, 125404 (2004).

**TABLE**

**Table I.** Calculated structural parameters of the fully relaxed perfect and deformed SWGT (5, 3) in a  $20 \text{ \AA} \times 20 \text{ \AA} \times C_l \text{ \AA}$  hexagonal supercell. The parameters (a, b, c) are defined as in Fig. 1(a).

And  $E_b$  is the binding energy per gold atom.

<i>(5,3) tube</i>	<i>Diameter (<math>\text{\AA}</math>) (relaxed)</i>	<i>lattice constant <math>C_l</math> (relaxed)</i>	<i>a (<math>\text{\AA}</math>)</i>	<i>b (<math>\text{\AA}</math>)</i>	<i>c (<math>\text{\AA}</math>)</i>	<i><math>E_b</math> (eV) per atom</i>
Perfect	4.23	20.758	2.835	2.819	2.754	-2.598
Stretched 0.05	4.15	21.796	2.848	2.794	2.889	-2.565
Stretched 0.1	4.04	22.834	2.851	2.754	3.024	-2.501
Torsion $+1.006^\circ$	4.27	17.825	2.821	2.853	2.731	-2.606
Torsion $+4.302^\circ$	4.32	12.327	2.762	2.930	2.744	-2.583
Torsion $-6.562^\circ$	4.31	2.709	3.010	2.756	2.709	-2.567
Shear 0.0314	4.27	17.826	2.821	2.853	2.731	-2.606

**Table II.** Energy gap versus tube length for the finite SWGT (5, 0).

The original length of tube (nm)	1.5	2.0	2.5	3.0	3.5	4.0	4.5
The optimized length of tube (nm)	1.37	1.83	2.29	2.75	3.2	3.67	4.12
Semiconductor (S) or Metal (M)	S	S	S	M	S	S	M
Energy gap (eV)	0.75	0.3	0.16	0.0	0.23	0.165	0.0

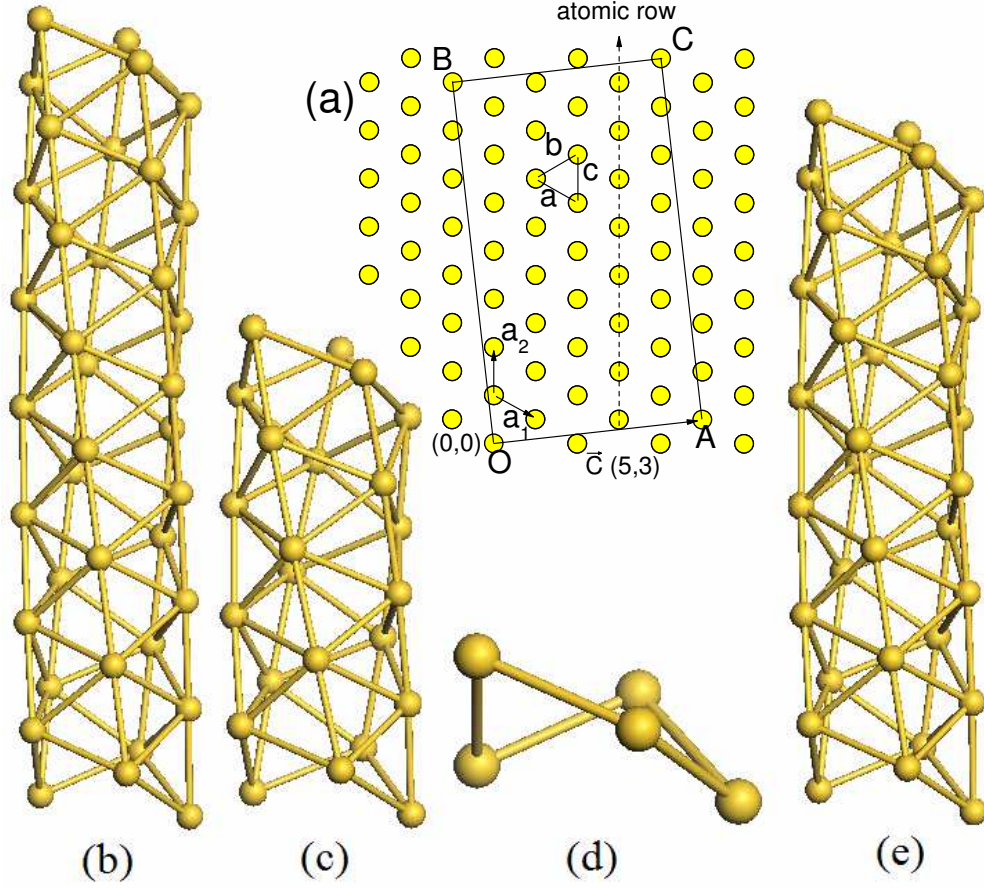


FIG. 1: (Color online) (a) The triangular network sheet of gold atoms forming the SWGT. The nearest neighbor distance between two gold atoms is chosen to be 2.9 Å. Ball-and-stick model of one unit cell for the 4 Å diameter SWGT (5, 3): (b) undeformed structure with its total atom number of 38; (c) torsional strain of  $+4.302^\circ$  (23 atoms); (d) torsional strain of  $-6.562^\circ$  (5 atoms); (e) shear strain of 0.0314 (33 atoms).



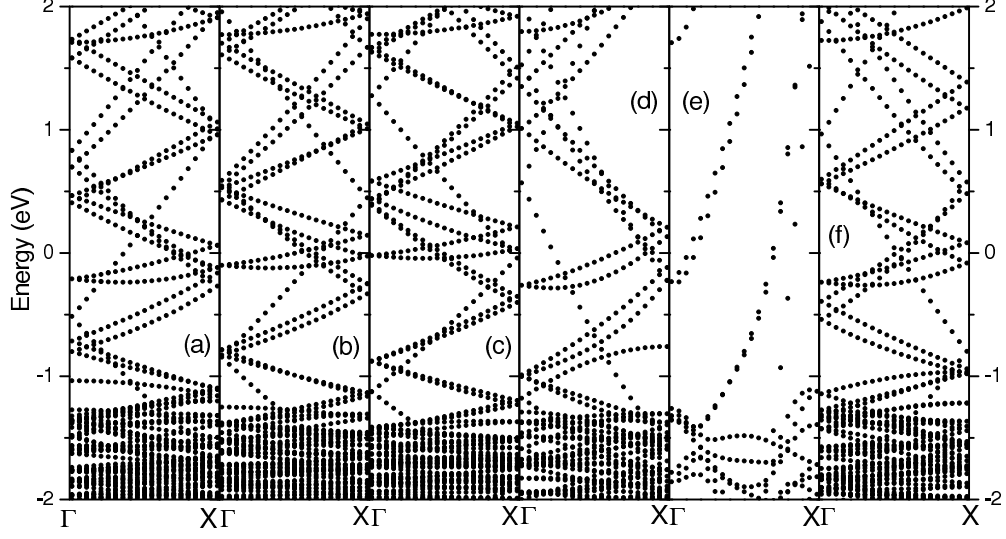


FIG. 2: Calculated band structures of : (a) perfect SWGT (5, 3); (b), (c), (d), (e) and (f) deformed ones, respectively, under uniaxial stretch strain of 0.05 and 0.1, torsional strain of  $+4.302^\circ$  and  $-6.562^\circ$ , and shear strain of 0.0314. The Fermi level is set at zero.

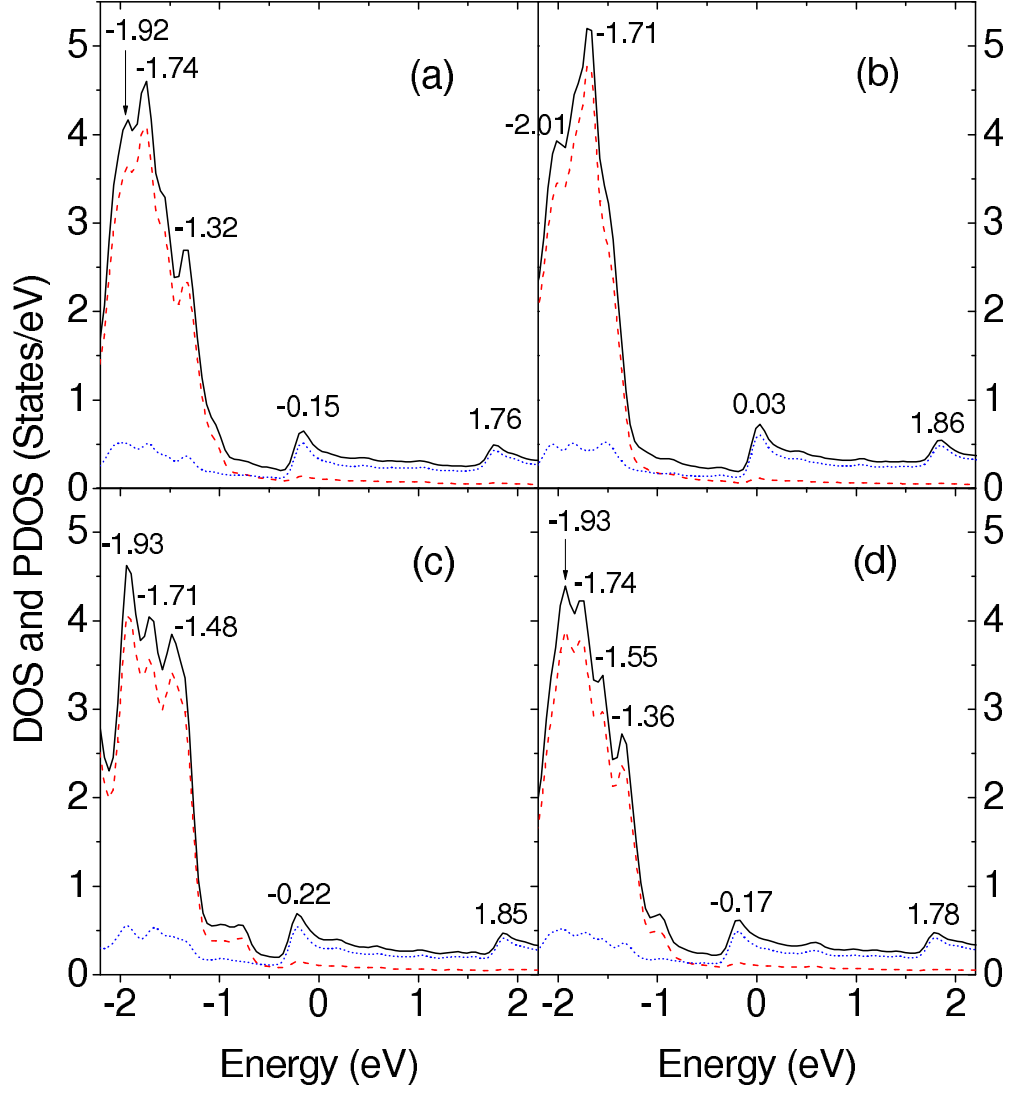


FIG. 3: (Color online) Calculated total DOSs (solid line), PDOSs for  $d$  electrons (dash line) and  $s$  electrons (dot line): (a) perfect SWGT (5, 3), (b), (c) and (d) deformed ones, respectively, under uniaxial strain of 0.1, torsional strain of  $+4.302^\circ$ , and shear strain of 0.0314. The Fermi level is set at zero.

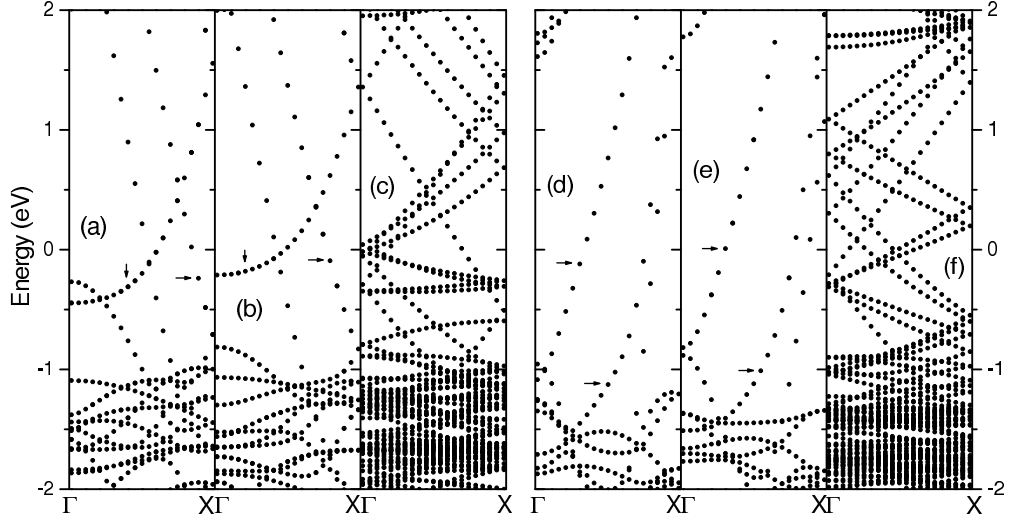


FIG. 4: Calculated band structures of : (a) perfect SWGT (5, 0) (10 atoms); (b) and (c) deformed ones, respectively, under uniaxial stretch strain of 0.1, torsional strain of  $+4.715^\circ$  (35 atoms); (d) perfect SWGT (6, 3) SWGT (6 atoms); (e) and (f) deformed ones, respectively, under uniaxial stretch strain of 0.1, torsional strain of  $+6.587^\circ$  (45 atoms). The Fermi level is set at zero.